Measurement of the Cross Section for W and Z Production to Electron Final States with the DØ Detector at $\sqrt{s} = 1.96$ TeV

The DØ Collaboration
URL http://www-d0.fnal.gov
(Dated: August 12, 2004)

Preliminary measurements have been made of the W and Z boson production cross sections times branching fractions into electrons using the DØ detector and an integrated luminosity of 177.3 pb^{-1} of $p\bar{p}$ collisions from RunII of the Tevatron. The measured cross sections are:

$$\sigma_W \times B(W{\to}e\nu) = 2865.2 \pm 8.3(\text{stat}) \pm 62.8(\text{sys}) \pm 40.4(\text{pdf}) \pm 186.2(\text{lumi}) \text{ pb}$$
$$\sigma_Z \times B(Z{\to}ee) = 264.9 \pm 3.9(\text{stat}) \pm 8.5(\text{sys}) \pm 5.1(\text{pdf}) \pm 17.2(\text{lumi}) \text{ pb}$$

The ratio R of the W cross section times branching fraction to the Z cross section times branching fraction is $10.82 \pm 0.16(\text{stat}) \pm 0.25(\text{sys}) \pm 0.13(\text{pdf})$.

Preliminary Results for Summer 2004 Conferneces

I. INTRODUCTION

Measurement of the production cross sections multiplied by the leptonic branching fractions (σB) for W and Z bosons can be used to test predictions of QCD for W and Z production. The ratio, R, of the measured σB values can be used to indirectly determine the width of the W boson.

In this paper, preliminary measurements of $\sigma_W B(W \to e\nu)$ and $\sigma_Z B(Z \to ee)$ are reported, using data obtained with the DØ detector in Run II of the Fermilab Tevatron using $p\bar{p}$ collisions at $\sqrt{s} = 1.96$ TeV. Data were collected between September 2002 and Septemeber 2003 corresponding to 177.3 ± 11.5 pb^{-1} of collisions. Analysis details can be found in Ref. [1].

II. THE DØ DETECTOR

The main elements of the DØ detector [2] used in this measurement are the liquid-argon/uranium calorimeter and the central-tracking system, which consists of a silicon microstrip tracker (SMT) and a central fiber tracker (CFT), both located within a 2 T superconducting solenoidal magnet. The calorimeter consist of three sections: a central section (CC) covering $|\eta|$ up to ≈ 1, and two end calorimeters (EC) extending coverage to $|\eta| \approx 4$, all housed in separate cryostats [3]. The SMT has $\approx 800,000$ individual strips, with typical pitch of $50 - 80$ μm, and a design optimized for tracking and vertexing capability at pseudorapidities of $|\eta| < 3$. The system has a six-barrel longitudinal structure, each with a set of four layers arranged axially around the beam pipe, and interspersed with 16 radial disks. The CFT has eight thin coaxial barrels, each supporting two doublets of overlapping scintillating fibers of 0.835 mm diameter, one doublet being parallel to the collision axis, and the other alternating by $\pm 3°$ relative to the axis. Luminosity is measured using plastic scintillator arrays located in front of the EC cryostats, covering $2.7 < |\eta| < 4.4$.

The trigger and data acquisition systems are designed to accommodate the high luminosities of Run II. Based on preliminary information from tracking, calorimetry, and muon systems, the output of the first level of the trigger is used to limit the rate for accepted events to ≈ 1.5 kHz. At the next trigger stage, with more refined information, the rate is reduced further to ≈ 800 Hz. These first two levels of triggering rely mainly on hardware and firmware. The third and final level of the trigger, with access to all the event information, uses software algorithms and a computing farm, and reduces the output rate to ≈ 50 Hz, which is written to tape.

III. DATA SELECTION

W and Z boson production is characterized, respectively, by the presence of a high transverse energy electron and large missing transverse energy, or by two high transverse energy electrons.

A. Electron Identification

Electrons are initially identified as an electromagnetic (EM) cluster found in the central calorimeter using a simple cone algorithm. To reduce background contamination (mostly from jets faking electrons) in the sample, electron candidates are required to have a large fraction of their energy deposited in the EM section of calorimeter and pass energy isolation and shower shape requirements. To ensure that candidates impact regions of the calorimeter where the electromagnetic energy scale of the calorimeter is well measured, the central position of candidates is required lie well within the fiducial region of the central calorimeter and away from module boundaries. Electron candidates are classified as *tight* if a track is matched spatially to it and if the track transverse momentum is close to the transverse energy of the EM cluster.

B. Event Selection

Z boson candidate events are required to have at least two electron candidates with transverse energy greater than 25 GeV and $|\eta| < 1.05$, corresponding to the highest efficiency and acceptance region of the calorimeter and tracking system. At least one of the electrons must be associated with the electromagnetic object that fired the trigger(s) for the event. At least one of the electron candidates is required to be tight (have a track matched to it) to reduce QCD background contamination. The invariant mass of the two electrons must be near the nominal mass of the Z boson within 70 and 110 GeV. A total of 4712 Z candidates are found.

W candidates are required to have at least one electron candidate with transverse energy greater than 25 GeV and $|\eta| < 1.05$. The electron is required to have fired the trigger for the event. The missing transverse energy in the event, measured from the vector sum of all the calorimeter cell energies, is required to be greater than 25 GeV. A total of 175572 candidates are found.

IV.   BACKGROUND SUBTRACTION

The main background to both W and Z production is from QCD processes that produce jets in the final state that fake the signature of an electron in the DØ detector. This background is subtracted using statistical methods as described below.

The largest remaining background to $Z \to ee$ production comes from $Z \to \tau\tau$. Since both taus must decay to electrons, the resulting background is negligible.

For $W \to e\nu$ production, the largest remaining backgrounds comes from $W \to \tau\nu$ and $Z \to ee$ processes. These backgrounds are estimated using the MC generator PYTHIA [4] and a full GEANT-based simulation of the DØ detector. Background fractions from these processes are estimated to be $(1.25 \pm .03)\%$ and $(0.26 \pm 0.05)\%$ for $W \to \tau\nu$ and $Z \to ee$ respectively.

A.   QCD Background in Z Candidates

The QCD background is subtracted by fitting a signal shape from PYTHIA plus an estimate of the background shape to the invariant di-electron mass distribution of the Z boson candidates. The shape of the background distribution is determined from data events with two electron candidates that fail a loose shower shape requirement. The scaled background shape distribution is subtracted from the Z boson candidate distribution. The number of Z candidates after background subtraction is 4624.9 ± 68.0.

B.   QCD Background in W Boson Candidates

In order to subtract QCD background from the number of W candidates two linear equations are constructed using the number of W candidates with and without requiring a track match to the electron candidate. The equations are solved for the *true* number of W bosons produced:

$$N_{Wcand} = N_W + N_{QCD}$$

$$N_{Wcand}^{track} = \epsilon^{track} N_W + f_{QCD} N_{QCD}$$

Yielding

$$N_W = \frac{N_{Wcand}^{track} - f_{QCD} N_{Wcand}}{\epsilon_{track} - f_{QCD}}$$

where N_W is the true number of W bosons, N_{Wcand} is the total number of W candidate events, N_{Wcand}^{track} is the number of W candidate events with a track matched to the electron. The fake track match probability, f_{QCD}, is the probability that a fake electron from a jet in a QCD event has a track matched to it. ϵ_{track} is the efficiency of finding a track matched to a true electron in a signal event. Both f_{QCD} and ϵ_{track} are measured from data as described in the next sections. The track match efficiency and and track match fake probability have a strong dependence on the position of the electron in the calorimeter and on the location of the event vertex. Therefore, the above equations are applied in bins of these quantities. The number of W candidates after background subtraction is 116569 ± 341.

Fake Track Match Probability

Fake track match probability is determined using a sample of di-jet events from data. Exactly two jets are required and must be back-to-back to reduce the contamination of W+jet events. One jet is required to have a low EM energy fraction and the other is required to pass all the electron identification requirements. The ratio of events in this sample where the electron-like jet also has a track matched to it gives the fake track match probability. The average measured fake track match probability is approximately $(1.64 \pm 0.66)\%$.

V. EFFICIENCY MEASUREMENTS

Efficiencies of the trigger, electron identification (including initial reconstruction), and track match requirements are determined from the data sample. Z boson candidate events are selected requiring two tight electrons, with the exception that one of the electrons (the *probe* electron) does not have to pass the requirement under study. The efficiency of the requirement is simply the fraction of events where the probe electron *does* pass the requirement. Using this method, the efficiencies are determined with respect to the electron transverse energy, electron position, and primary vertex position. The average measured trigger, electron identification, and track-match efficiencies are $(98.2 \pm 0.6)\%$, $(91.7 \pm 1.4)\%$, and $(79.0 \pm 0.5)\%$ respectively.

VI. MONTE CARLO SIMULATION

Acceptance of the geometric and kinematic cuts is determined from a parameterized Monte Carlo simulation (PMCS). Using PYTHIA, samples of $Z/\gamma^* \to ee$ and $W \to e\nu$ events were generated with the CTEQ6 LO PDF [5]. For each event, the measured energy response of the DØ calorimeter is applied to the final state electrons and in the case of W boson production to the hadronic recoil vector. Additionally, the measured single electron trigger, electron identification, and track-match efficiencies are applied to the final state electrons. Figure 1 compares the PMCS result to the invariant mass of electron pairs in the Z boson candidate data sample. Figures 2, 3, and 4 show the comparison to the W boson candidate sample with respect to relevant kinematic variables and the measured transverse mass of the W boson. The data are reasonably described by the simulation. Discrepancies arise mostly from uncertainties in the modeling of the detector response, the effects of which are accounted for when assigning a systematic uncertainty to the final measurement.
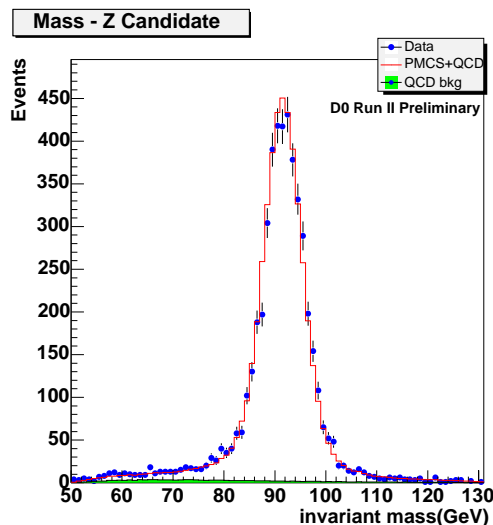

FIG. 1: The invariant mass of electron pairs in Z boson candidate events. The estimated QCD background and Monte Carlo simulation are normalized to fit the data.

VII. UNCERTAINTY ESTIMATES

The significant sources of uncertainty and their estimated effect on the measured cross sections and the ratio are summarized in Table I. The uncertainty due to the uncertainty on the PDFs input into PMCS is determined using the method prescribed by the CTEQ collaboration [5].

The largest uncertainty on the cross section measurements comes from the uncertainty on the luminosity measurement, which cancels when determining the ratio of the W boson to Z boson production cross section. The largest contribution to the uncertainty of the ratio comes from the uncertainty on the electron identification efficiency and the uncertainty assigned to the Monte Carlo simulation. The uncertainty of the simulation is dominated by the uncertainties on the energy scale and energy resolution of the calorimeter.
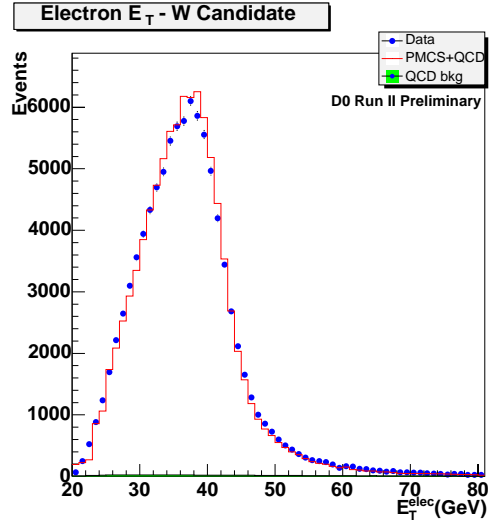
FIG. 2: The transverse energy of electrons in W boson candidate events with a track matched to the electron.
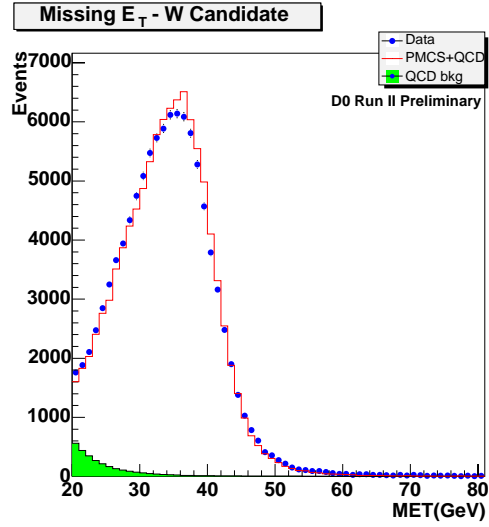

FIG. 3: The missing transverse energy in W boson candidate events with a track matched to the electron.

VIII.   RESULTS

The W and Z cross sections time branching ratios are calculated using

$$\sigma_Z \times B(Z{\rightarrow}ee) = \frac{N_Z}{\mathcal{L}} \frac{1}{A_Z} (1 - f_{DY}^Z)$$

$$\sigma_W \times B(W{\rightarrow}e\nu) = \frac{N_W}{\mathcal{L}} \frac{1}{A_W} (1 - f_\tau^W - f_Z^W)$$

$$R = \frac{\sigma_W \times B(W{\rightarrow}e\nu)}{\sigma_Z \times B(Z{\rightarrow}ee)} = \frac{N_W}{N_Z} \frac{A_Z}{A_W} \frac{1 - f_\tau^W - f_Z^W}{1 - f_{DY}^Z}$$

where N_W and N_Z are the number of W and Z events after background subtraction; $\mathcal{L}$ is the integrated luminosity for the data sample; f_{DY}^Z is the Drell-Yan contribution in $Z \rightarrow ee$ events, and is the ratio of the $Z \rightarrow ee$ to the $Z/\gamma^* \rightarrow ee$ cross section with in the acceptance of the measurement as calculated by PYTHIA; f_τ^W is the fraction
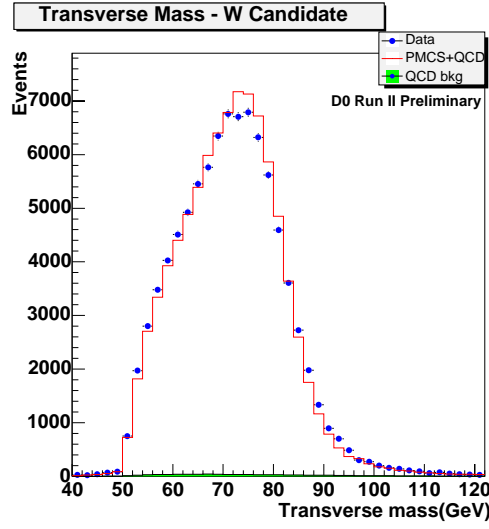
FIG. 4: The transverse mass of the W boson in W boson candidate events with a track matched to the electron.

	Relative Uncertainty (%) on		
Source	σ_W	σ_Z	R
stat			
Number of Events	0.29	1.47	1.50
sys			
Stat. Error on Efficiencies	0.72	0.77	0.58
Background Subtraction	0.35	0.82	0.47
Fake Track Match Prob.	0.45	n/a	0.45
PMCS Parameters	1.13	0.84	1.41
Trigger Eff	0.59	0.06	0.53
Electron ID Eff.	1.43	2.86	1.43
Track Match Eff.	0.52	0.35	0.17
Total **sys**	2.19	3.21	2.27
pdf			
PDF (CTEQ Method)	1.41	1.94	1.21
lumi			
Luminosity	6.5	6.5	n/a

TABLE I: Summary of sources of uncertainties. All values are relative and given in percent. n/a = Not Applicable

of $W \rightarrow \tau\nu$ events that pass the $W \rightarrow e\nu$ selection criteria; and f_Z^W is the fraction of Z boson events misidentified as W bosons. A_W and A_Z are the acceptance values for W and Z bosons determined from the parameterized Monte Carlo simulation. The acceptance values include the trigger efficiency, electron identification efficiency, and (for A_Z) the track match efficiency.

The measured cross sections are:

$$\sigma_Z \times B(Z \rightarrow ee) = 264.9 \pm 3.9 (\text{stat}) \pm 8.5 (\text{sys}) \pm 5.1 (\text{pdf}) \pm 17.2 (\text{lumi}) \text{ pb}$$
$$\sigma_W \times B(W \rightarrow e\nu) = 2865.2 \pm 8.3 (\text{stat}) \pm 62.8 (\text{sys}) \pm 40.4 (\text{pdf}) \pm 186.2 (\text{lumi}) \text{ pb}$$
$$R = \frac{\sigma_W \times B(W \rightarrow e\nu)}{\sigma_Z \times B(Z \rightarrow ee)} = 10.82 \pm 0.16 (\text{stat}) \pm 0.25 (\text{sys}) \pm 0.13 (\text{pdf})$$

Acknowledgments

[1] D. Chapin *et al.*, "Measurement of $Z \to ee$ and $W \to e\nu$ Production Cross Sections with $|\eta| < 2.3$", DØNote #4403 (2004).
[2] V. Abazov, et al., in preparation for submission to Nucl. Instrum. Methods Phys. Res. A, and T. LeCompte and H.T. Diehl, "The CDF and DØ Upgrades for Run II", Ann. Rev. Nucl. Part. Sci. **50**, 71 (2000).
[3] S. Abachi, *et al.*, Nucl. Instrum. Methods Phys. Res. A **338**, 185 (1994).
[4] T. Sjöstrand *et al*, Computer Physics Comm. **135**, 238 (2001).
[5] J. Pumplin *et al*, J.H.E.P. **207**, 012 (2002).

APPENDIX A: COMPARISON TO SM AND TEVATRON RESULTS

The SM prediction of the cross section times branching fraction with respect to the center-of-mass energy is compared to the measurement in Figs. 5 and 6.
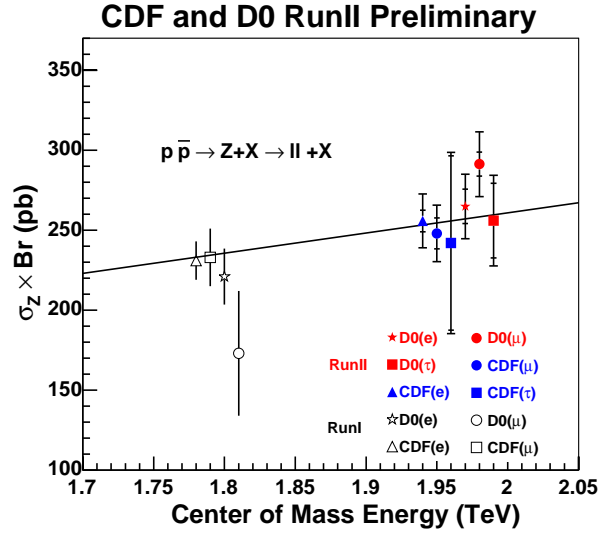

FIG. 5: Recent measurements of the $Z \to \ell\ell$ cross section times branching fraction. The inner (outer) error bars on the data points exclude (include) the uncertainty from the luminosity measurement.
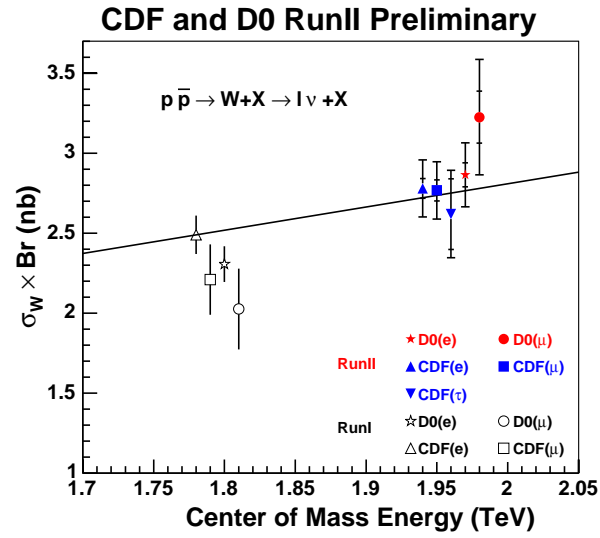

FIG. 6: Recent measurements of the $W \to \ell\nu$ cross section times branching fraction. The inner (outer) error bars on the data points exclude (include) the uncertainty from the luminosity measurement.